

# The dynamics of premixed flames propagating in non-uniform velocity fields: Assessment of the significance of intrinsic instabilities in turbulent combustion

By S. Kadowaki<sup>†</sup>, S.H. Kim AND H. Pitsch

## 1. Motivation and objectives

Emissions of greenhouse gases and air pollutants are induced principally primarily by the combustion of fossil fuels. To reduce emissions of carbon dioxide and nitrogen oxide, lean combustion of hydrogen-air and/or methane-air mixtures is often adopted. Since hydrogen and methane are lighter than air, i.e. the mass diffusion of the deficient reactant is in excess of the heat diffusion, hydrogen-air and methane-air lean premixed flames are usually unstable. Instabilities of premixed flames are observed in experiments as the formation and unstable behavior of cellular flames (Clavin 1985; Law 1988; Hertzberg 1989; Sivashinsky 1990; Kadowaki & Hasegawa 2005). The intrinsic instabilities of premixed flames are hydrodynamic instabilities caused by the thermal expansion through the flame front, and diffusive-thermal instabilities caused by the preferential diffusion of mass versus heat. Through numerical simulations, it was found that the shape and motion of premixed flames are strongly influenced by intrinsic instabilities (Kadowaki & Hasegawa 2005). Moreover, the characteristics of cellular flames generated by intrinsic instabilities have been numerically investigated in detail by several researchers (Patnaik & Kailasanath 1994; Denet & Haldenwang 1995; Bychkov *et al.* 1996).

Premixed-type gas turbines, often burning methane or possibly hydrogen, are extensively adopted in industry because of low carbon dioxide and nitrogen oxide emissions. To control combustion in premixed-type gas turbines, the knowledge of turbulent premixed flames under high-pressure and high-temperature conditions is indispensable. Under these conditions, the flame thickness becomes smaller, and consequently, the level and significance of intrinsic instabilities increase. To control hydrogen-air and/or methane-air lean premixed combustion to high-load combustors, an understanding of the influence of intrinsic instabilities on turbulent flames is further required. It was reported that the characteristics of turbulent premixed flames are significantly influenced by intrinsic instabilities under high pressure and high temperature conditions (Kobayashi *et al.* 2004). Numerical simulations can investigate these interactions of turbulent combustion and intrinsic instabilities. The results from these simulations can further be used to construct models for Reynolds averaged combustion models and large-eddy simulations.

The combined effects of the intrinsic instabilities and velocity disturbances on the dynamics of premixed flames have been usually studied in simplified systems. Cambray & Joulin (1992) performed calculations of premixed flames propagating in disturbed velocity fields on the basis of the diffusive-thermal model equation and showed that the unstable behavior of flame fronts is influenced by the Lewis number, i.e., by intrinsic instabilities.

<sup>†</sup> Nagaoka University of Technology Japan.

Their numerical results are, however, valid only for premixed flames with sufficiently small heating value, which is due to the assumption of constant density. In the analytic study of strongly corrugated turbulent flames based on a nonlinear model equation, the burning velocity was shown to significantly increase due to the hydrodynamic instability when turbulence is moderate and the maximum hydrodynamic length scale is much larger than the cut-off scale of the instability (Bychkov 2003). The diffusive-thermal instability was not considered in Bychkov (2003). A systematic study on the effects of the intrinsic instabilities and velocity disturbances using the full Navier-Stokes equations has not been reported yet.

The inclusion of the intrinsic instabilities on modeling of turbulent premixed combustion has been a challenging topic. A simple criterion that the intrinsic instabilities are of significance in turbulent flames is  $u'/S_u < O(1)$ , where  $u'$  is the turbulent intensity and  $S_u$  is the laminar flame speed. Most combustion models neglect the instability effects based on this criterion and on the assumption of high turbulence intensity. However, the relative importance of the instabilities and turbulence is determined not only by the velocity scales but also by the length scales. Boughanem and Trouve (1998) proposed a turbulent combustion diagram in which the domain of the influence of intrinsic instabilities is shown. Their criterion was obtained by comparing a characteristic flame stretch due to flame instabilities and that due to turbulence.

In this paper, the combined effects of intrinsic instabilities and velocity disturbances on the dynamics of premixed flames are investigated to assess the significance of intrinsic instabilities in turbulent combustion. The unsteady simulations of premixed flames propagating in non-uniform velocity fields are performed based on the compressible Navier-Stokes equations. The relationship between the size of cells and the wavelength of the velocity disturbance is clarified. The effects of the intensity of disturbances and intrinsic instabilities on the burning velocity are also investigated. The significance of intrinsic instabilities in turbulent combustion is discussed and a simple regime diagram based on a linear theory is proposed.

## 2. Numerical procedure

The compressible two-dimensional Navier-Stokes equations are solved in conjunction with a reactive scalar and an energy equation. The physical parameters are chosen to simulate a gas mixture with an unstrained laminar burning velocity of 3.93 m/s and an adiabatic flame temperature of 2086 K. Although the present burning velocity is much larger than that of hydrocarbon-air premixed flames, it can represent hydrogen-oxygen premixed flames and it is sufficiently small compared with the speed of sound, so that the Mach number remains small. Thus, the non-dimensionalized numerical results are hardly influenced by the choice of the burning velocity.

In the present study, the interaction of intrinsic instabilities and velocity fluctuations is investigated. For this, velocity disturbances are superimposed on the a velocity field using the following inlet-velocity conditions:

$$\begin{aligned} u_u &= U + A \cos(2\pi y/\lambda_n), \quad \lambda_n = L_y/n \\ v_u &= 0 \end{aligned} \tag{2.1}$$

Here,  $U$  is the mean inlet-flow velocity,  $A$  is the amplitude of the velocity fluctuations,  $n$  is the wavelength,  $L_y$  is the length of the computational domain in the  $y$ -direction, and  $n$  is a positive integer. Outlet-flow conditions are provided by free-flow conditions.

Periodic conditions are used in the  $y$ -direction. All length scales are non-dimensionalized by the laminar flame thickness.

The numerical integration is performed using an explicit MacCormack scheme. The computational domain is  $600\delta$  in the  $x$ -direction, and  $\lambda_c$  to  $4\lambda_c$  in the  $y$ -direction, where  $\lambda_c$  is the critical wavelength at  $Le = 1.0$ . A stretched grid is used in the  $x$ -direction with a minimum grid spacing of a fifth of the preheat zone thickness. In the  $y$ -direction, a uniform grid is used with a grid spacing of  $\lambda_c/192$  at  $Le = 0.5$  and of  $\lambda_c/64$  at  $Le = 1.0$ . The time-step has been chosen to satisfy the CFL condition.

All calculations were performed on an SGI Origin 2000 computer at the Institute of Fluid Science at Tohoku University.

### 3. Results

#### 3.1. Dynamic behavior of premixed flames

The critical wavelength is the linearly most unstable wavelength and is obtained from the dispersion relation for premixed flames propagating in uniform velocity fields. The critical wavelength at  $Le = 0.5$  and  $1.0$  are  $11.5$  and  $34.1$ , respectively. Although the formation of cellular-flame fronts is only by intrinsic instabilities, because of non-linear effects, the cell size is not equal to the critical wavelength. Through the calculation of large computational domains, we have obtained the size of the average cell depending on the Lewis number (Kadowaki *et al.* 2004). The cell size is slightly larger than the critical wavelength at  $Le = 0.5$  and is about four times the critical wavelength at  $Le = 1.0$ .

Here, the dynamics of premixed flames propagating in non-uniform velocity fields are investigated. In the unburned gas region, the velocity disturbances decrease in downstream direction owing to viscous dissipation. The RMS of the velocity disturbance in front of the flame front is almost unity in this section. The wavelength of the velocity disturbance is fixed to the critical wavelength of the  $Le = 1.0$  flame ( $\lambda_n = \lambda_c = 34.1$ ).

First, the  $Le = 1.0$  case is considered. The behavior of premixed flames is influenced only by hydrodynamic instabilities in this case. Figure 1 shows the temperature and velocity distributions of the cellular flame in the computational domain with  $L_y = \lambda_c = 34.1$  at three different times ( $t = 110, 116$ , and  $118$ ). Owing to the velocity disturbance, a cellular flame front appears. The cell shape changes in time, alternating between a shallow cell ( $t = 110$  and  $118$ ) and a deep cell ( $t = 116$ ). This unstable behavior is not observed in  $Le = 1.0$  flames propagating in uniform and weakly disturbed velocity fields. Thus, the coupling of the hydrodynamic instabilities and the relatively strong velocity disturbance generates this behavior. The velocity distribution of the unburned gas ahead of the flame front is affected by the oscillating flame front, and hence changes with time, even though the velocity distribution at the upstream boundary is unchanged.

The behavior of the cellular flame in a larger computational domain,  $L_y = 4\lambda_c = 136.4$ , is shown in Fig. 2. At  $t = 50$ , the cellular flame is composed of four cells. The leading edge of cells corresponds to the minimum inlet velocity, and the trailing edge corresponds to the maximum. The initial evolution is primarily governed by the velocity disturbance. After that, cells combine together ( $t = 120$ ), and one large cell forms ( $t = 200$ ). The size of this large cell is almost equal to the average size of cellular flames generated only by intrinsic instabilities (Kadowaki *et al.* 2004). The cell depth is, however, larger than that of the uniform velocity field case, since the velocity disturbance brings about a more unstable cellular flame.

Next, the  $Le = 0.5$  case is considered. In this case, the behavior of premixed flames

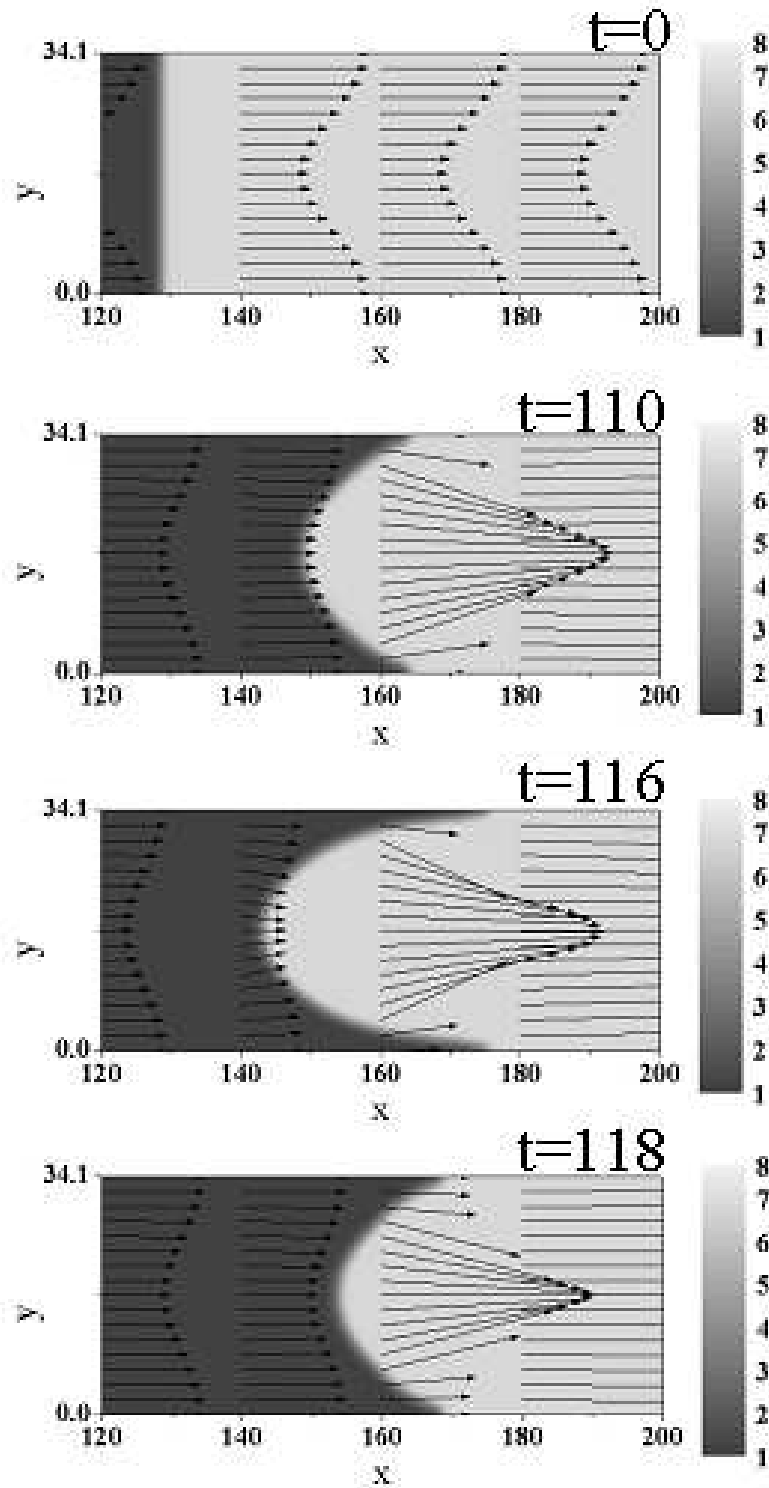


FIGURE 1. Behavior of the cellular flame at  $Le = 1.0$ ,  $L_y = 34.1$ ,  $\lambda_n = 34.1$ ,  $A = 2.2$ , and  $U = 2.5$  ( $t = 0, 110, 116$ , and  $118$ ).

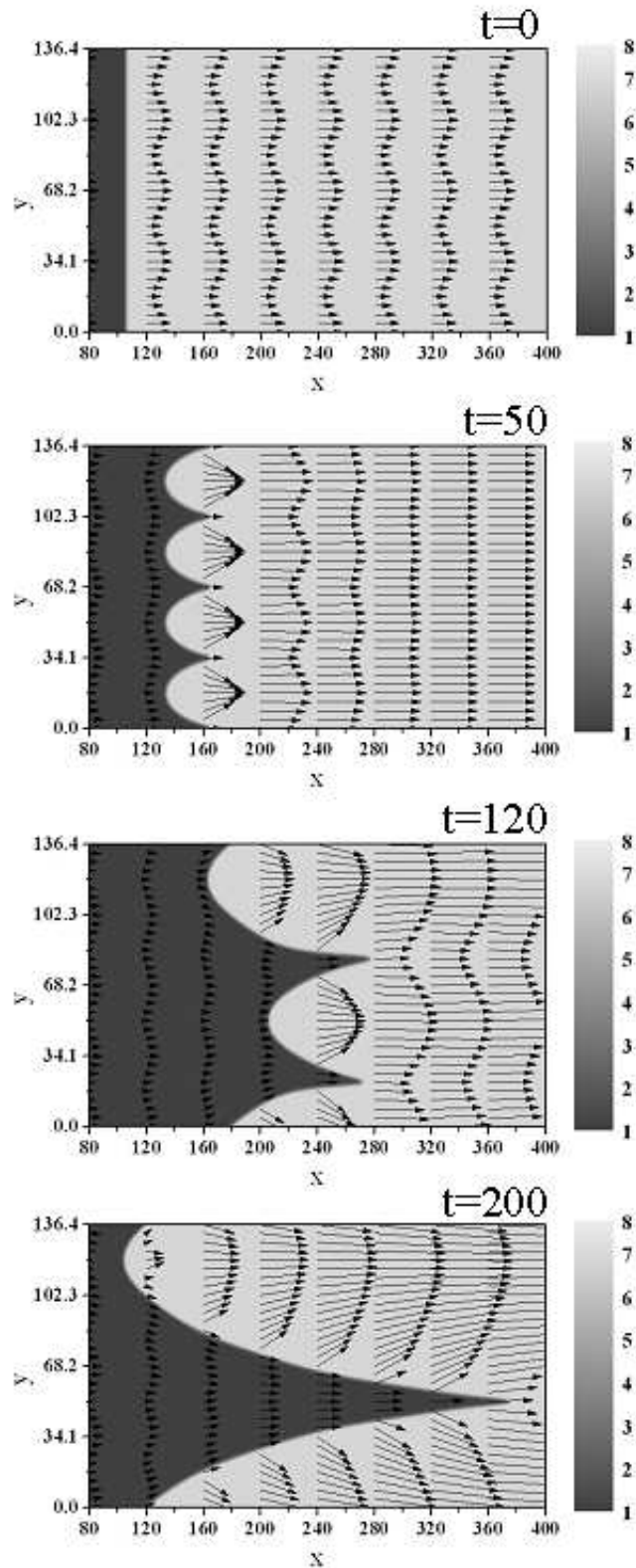


FIGURE 2. Behavior of the cellular flame at  $Le = 1.0$ ,  $L_y = 136.4$ ,  $\lambda_n = 34.1$ ,  $A = 2.2$ , and  $U = 3.0$  ( $t = 0, 50, 120$ , and  $200$ ).

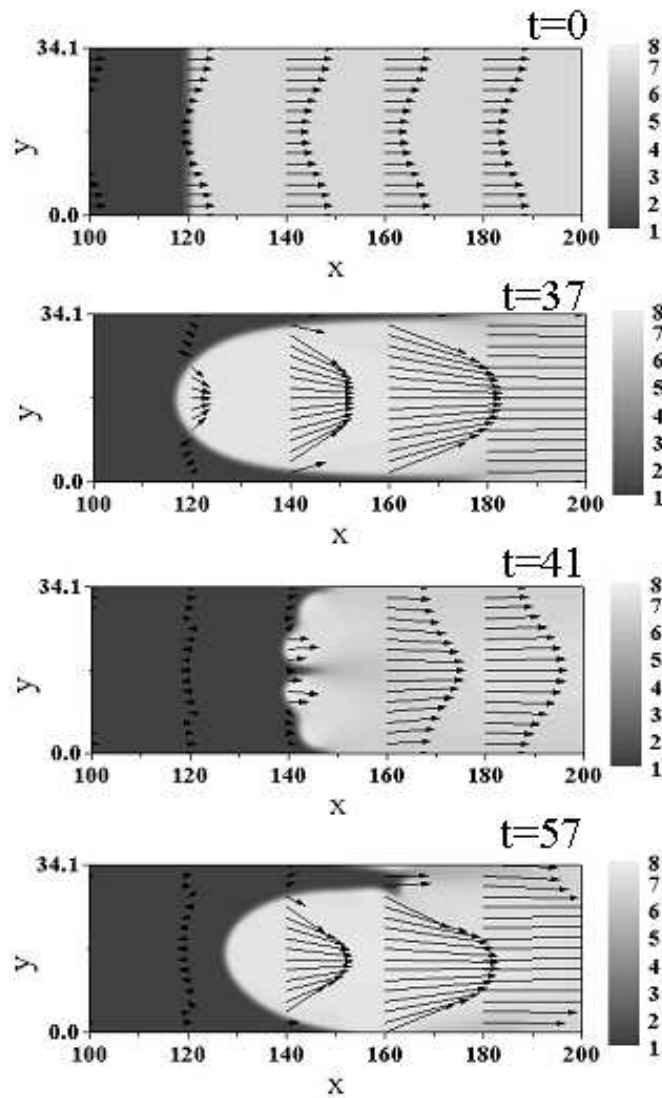


FIGURE 3. Behavior of the cellular flames at  $Le = 0.5$ ,  $L_y = 34.1$ ,  $\lambda_n = 34.1$ ,  $A = 2.5$ , and  $U = 3.2$  ( $t = 0, 37, 41$ , and  $57$ ).

is influenced by hydrodynamic and diffusive-thermal instabilities. Figure 3 shows the unsteady behavior of the cellular flame in the computational domain with  $L_y = \lambda_c = 34.1$ . The cellular flame oscillates dynamically, and a large cell ( $t = 37$  and  $57$ ) and small cells ( $t = 41$ ) appear alternately. Small cells appear, because the cell size of the intrinsic instabilities ( $= 11.5$ ) is smaller than the wavelength of the velocity disturbance ( $= 34.1$ ).

The unsteady behavior in a larger computational domain,  $L_y = 4\lambda_c = 136.4$ , is shown in Fig. 4. Similarly to the  $Le = 1.0$  flame, the initial development of the cellular flame is primarily governed by the velocity disturbance, while small cells are observed at the trailing edge ( $t = 54$ ). After that, a division of cells is observed, and small cells are side by side ( $t = 57$ ). Cells combine together, and four cells appear again ( $t = 64$ ). After this

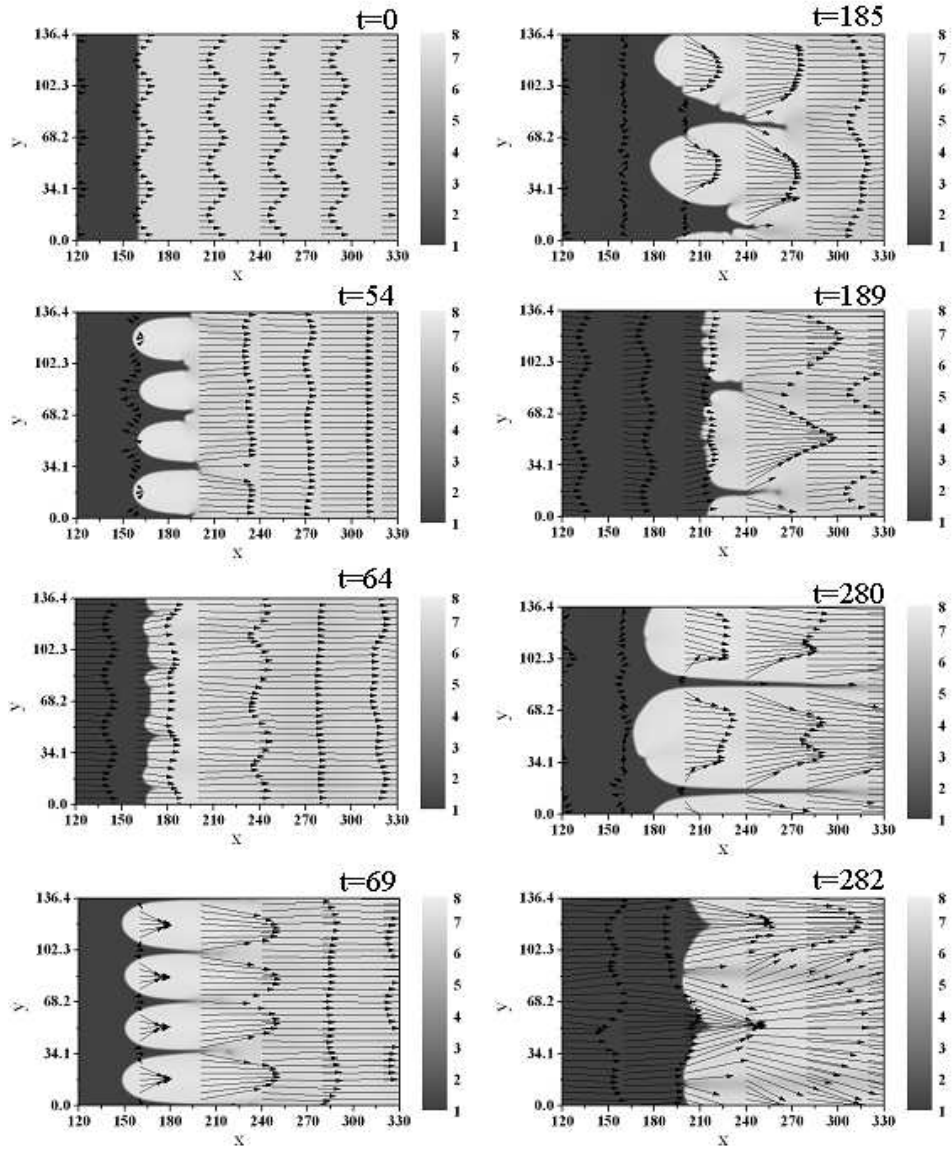


FIGURE 4. Behavior of the cellular flames at  $Le = 0.5$ ,  $L_y = 136.4$ ,  $\lambda_n = 34.1$ ,  $A = 2.5$ , and  $U = 3.0$  ( $t = 0, 54, 64, 69, 185, 189, 280$ , and  $282$ ).

repetition, cells of the wavelength of the velocity disturbance combine together, and two large cells appear, on which small cells are superimposed ( $t = 185$ ). The cusps of the large cells disappear, and small cells are side by side ( $t = 189$ ). After that, again two large cells are observed ( $t = 280$ ). This unsteady behavior of the cellular-flame front, i.e., the combination of small cells, evolution of large cells, disappearance of large cusps, and appearance of small side-by-side cells, is repeated.

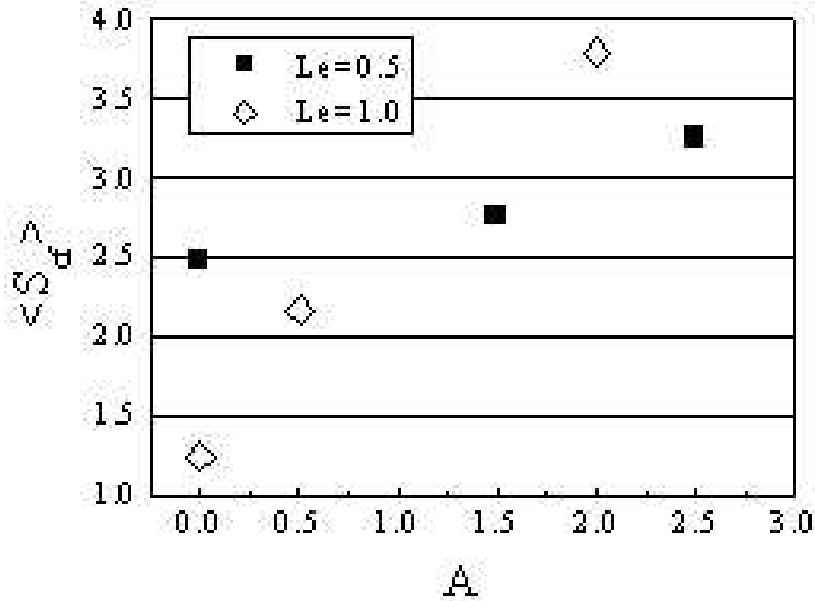


FIGURE 5. Averages of burning velocities at  $Le = 0.5$  and  $1.0$ , and  $L_y = 136.4$  as a function of the intensity of disturbance.

### 3.2. Burning velocity of cellular flames

The burning velocity of premixed flames propagating in non-uniform velocity fields is larger than that of planar flames, due to the cellular structure. In this section, the effects of the intensity of disturbances and intrinsic instabilities on the burning velocity of cellular flames are investigated. In the present calculation, integrating the reaction rate over the whole computational domain, and normalizing this by the corresponding value for planar flames yields the average enhanced burning velocity. The normalized value is consistent with the non-dimensional burning velocity typically defined for cellular flames.

The effect of intensity of the velocity disturbances on the burning velocity has been investigated by changing the amplitude of the disturbances. Figure 5 shows the averaged burning velocities at  $Le = 0.5$  and  $1.0$  as function of the velocity amplitude from the simulations using the large computational domain,  $L_y = 136.4$ . As the intensity increases, the burning velocity increases monotonically. The dependence of the burning velocity on the intensity is strongly influenced by the Lewis number. However, the shape and evolution of the flame is very similar at different velocity amplitudes. The burning velocity of  $Le = 1.0$  flames is found to depend much more strongly on the intensity. The wavelength of the velocity disturbances ( $= 34.1$ ) is smaller than the cell size ( $= 136.4$ ), so the flame-surface area is strongly affected by disturbances. Thus, the burning velocity increases more strongly because the velocity fluctuations are more effective in increasing the flame surface.

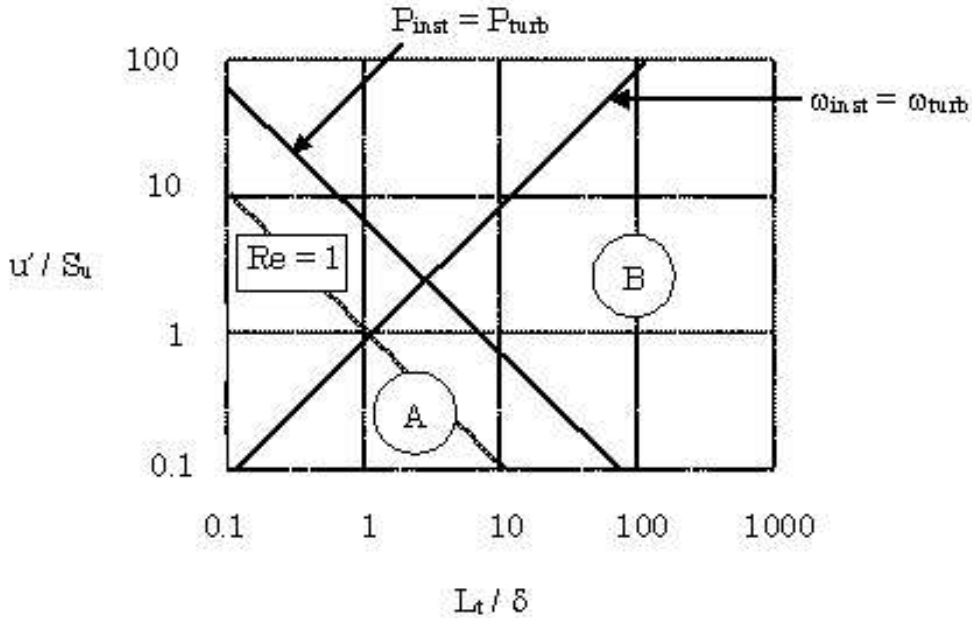


FIGURE 6. Regime diagram characterizing the relative significance of intrinsic instabilities in turbulent combustion.

#### 4. Discussion and regime diagram

The relative significance of intrinsic instabilities on the evolution of turbulent premixed flames can be identified by comparing the growth rate  $\omega$  and production rate  $P$  of flame fronts due to intrinsic instabilities and turbulence. Boughanem and Trouve(1998) have proposed a regime diagram where the growth rates of the instabilities are compared with the growth rates of the turbulence. However, the growth rate only provides the relative change of the flame surface irrespective of the length scale. Although the growth rates of these processes might be important for the dynamics of the flame, for an effective burning velocity, as defined in the previous section, the production rate of flame surface is more relevant. Therefore, we will here compare both the growth rate and the production rate of flame surface of both the intrinsic instabilities and the turbulence.

The growth rate  $\omega_{inst}$  and production rate  $P_{inst}$  due to intrinsic instability are defined as follows (Kadowaki *et al.* 2004):

$$\omega_{inst} = \frac{1}{l} \frac{dl}{dt}, P_{inst} = \frac{dl^2}{dt} \quad (4.1)$$

where  $l$  is the length between disturbed and non-disturbed flame fronts, and  $t$  is the time. In estimating the significance of intrinsic instabilities, we adopt the maximum growth rate and the maximum production rate, which have both been obtained from earlier simulations. These maximum quantities are determined as the function of the burning velocity and the preheat zone thickness. The growth rate  $\omega_{turb}$  and production rate  $P_{turb}$  due to turbulence can be expressed as (Pitsch 2005)

$$\omega_{turb} = c_1 \frac{u'}{L_t}, P_{turb} = 2c_1 u' L_t \quad (4.2)$$

where  $u'$  is the turbulence intensity and  $L_t$  is the integral scale of turbulence. The unknown constant  $c_1$  is assumed to be unity. Note that the expressions for the intrinsic instabilities here are taken from linear theory. The non-linear behavior leads to quantitatively different, but qualitatively the same behavior.

Using relationships (4.1) and (4.2), the regime diagram characterizing the relative significance of intrinsic instabilities in turbulent combustion can be constructed. This diagram is shown in Fig. 8. In constructing the regime diagram, the Lewis number is set to 0.5. In addition to (4.1) and (4.2), the line that  $L_t = \lambda_m = 5$  is shown in the diagram, where  $\lambda_m$  is the marginal wavelength. Since the instabilities do not grow below  $\lambda_m$ , the region of significance of the interactions of the instabilities with turbulence is limited to the right side of this line. For smaller turbulent length scales, the instabilities might still be important for the flame dynamics, but occur on a scale larger than the largest scale of the turbulence. In Region (A), where the contribution of intrinsic instabilities to the growth rate and production rate is greater than the contribution by turbulence, intrinsic instabilities have a crucial influence on the phenomena of turbulent premixed flames, i.e., the dynamic behavior of flame fronts and the increase of turbulent burning velocity. In Region (B), the growth rate due to intrinsic instabilities is larger than that due to turbulence, while the production rate of the flame surface is dominated by turbulence. The reason for this seemingly contradictory behavior is that the growth rate only describes the relative increase of flame surface. Since in this region, the flame surface production by turbulence occurs on a scale much larger than the critical wavelength of the turbulence, even a relatively smaller growth rate due to the turbulence leads to an larger absolute production of flame surface. The burning velocity of the flame is then primarily determined by the turbulence, although the dynamic behavior of the flames at the smaller scales can be affected by the intrinsic instabilities. Hence, the surface production at the scales comparable to the critical wavelength is dominated by the instabilities, which therefore control the small-scale dynamics of the flame. This behavior has been experimentally found by Kobayashi *et al.* (2004). In other regions, intrinsic instabilities have only a minor influence, and the effects of turbulence are dominant.

The regime diagram in Fig. 6 is based on the linear stage of the intrinsic instabilities of laminar flames. The domain of significance of the intrinsic instabilities can thus change due to the nonlinear effects and especially due to the departure from the laminar flame structure. For example, in the thin reaction regime, where transport in the preheat zone is governed by small scale turbulence, the diffusive-thermal instability is not important, because the effective Lewis number is close to unity. The cut-off scale of the hydrodynamic instability can also be changed due to thickening of the preheat zone.

## 5. Concluding remarks

We have performed two-dimensional unsteady calculations of reactive flows, based on the compressible Navier-Stokes equations to investigate the dynamics of premixed flames propagating in non-uniform velocity fields to assess the significance of intrinsic instabilities in turbulent combustion. Sinusoidal disturbances with a wavelength equal to the critical wavelength of the instability at  $Le = 1.0$  are superimposed on the velocity field of the unburned gas. The dynamic behavior of cellular flames is then generated by both the velocity disturbance and the intrinsic instabilities. When  $Le = 1.0$  and  $L_y = 4\lambda_c$ , the initial evolution is primarily governed by the velocity disturbance. After the initial evolution, the cells combine until one large cell appears. The size of the large cell is

almost equal to the average cell size of the cellular flames generated only by intrinsic instabilities without any velocity disturbances. When  $Le = 0.5$ , the cell size can be much smaller than the wavelength of the velocity disturbances. This is caused by the diffusive-thermal instabilities. The combination and division of cells is observed. The dynamics of premixed flames are drastically influenced not only by the velocity disturbances, but also by the intrinsic instabilities. The burning velocity of cellular flames propagating in non-uniform velocity fields is larger than that of planar flames. The increment in the burning velocity becomes larger as the intensity of disturbances becomes higher. The dependence of the burning velocity on the intensity is strongly influenced by the Lewis number. The average burning velocity of the  $Le = 1$  case is found to depend much more strongly on the velocity amplitude, because the wavelength of disturbances is smaller than the cell size, and as a consequence, the flame-surface area is more strongly affected.

Finally, a regime diagram is constructed to characterize the relative significance of intrinsic instabilities in turbulent combustion. The dynamic behavior of premixed flames is discussed in terms of growth rates and flame surface production rates. Two important regimes are identified. One regime, where the production of flame surface is dominated by the intrinsic instabilities, and another regime, where this quantity is dominated by the turbulence, but the instability has larger growth rates than the turbulence, and will therefore dominate the dynamics on the small scales of the size of the critical wavelength of the instability.

### Acknowledgment

S. K. wishes to thank Professor Parviz Moin for his hospitality during a stay at Stanford University through the Center for Turbulence Research Senior Visiting Fellow Program.

### REFERENCES

- BYCHKOV, V. V., GGOLBERG, S. M., LLIBERMAN, M. A. & ERIKSSON, L. E. 1996 Propagation of curved stationary flames in tubes. *Phys. Rev. E* **54**, 3713-3724.
- CAMBRAY, P. & JOULIN, G. 1992 On moderately-forced premixed flames. *Proc. Combust. Inst.* **24**, 61-67.
- CLAVIN, P. 1985 Dynamic behavior of premixed flame fronts in laminar and turbulent flows. *Prog. Energy Combust. Sci.* **11**, 1-59.
- DENET, B. & HALDENWANG, P. 1995 A numerical study of premixed flames Darrieus-Landau instability. *Combust. Sci. Technol.* **104**, 143-167.
- HERTZBERG, M. 1989 Selective diffusional demixing: occurrence and size of cellular flames. *Prog. Energy Combust. Sci.* **15**, 203-239.
- KADOWAKI, S., SUZUKI, H. & KOBAYASHI, H. 2004 The unstable behavior of cellular premixed flames induced by intrinsic instability. *Proc. Combust. Inst.* **30**, 169-176.
- KADOWAKI, S. & HASEGAWA, T. 2005 Numerical simulation of dynamics of premixed flames: flame instability and vortex-flame interaction. *Prog. Energy Combust. Sci.* **31**, 193-241.
- KOBAYASHI, H., SEYAMA, K., HAGIWARA, H. & OGAMI, Y. 2004 Burning velocity correlation of methane/air turbulent premixed flames at high pressure and high temperature. *Proc. Combust. Inst.* **30**, 827-834.
- LAW, C. K. 1988 Dynamics of stretched flames. *Proc. Combust. Inst.* **22**, 1381-1402.

- PATNAIK, G. & KAILASANATH, K. 1994 Numerical simulations of burner-stabilized hydrogen-air flames in microgravity. *Combust. Flame* **99**, 247-253.
- PITSCH, H. 2005 A consistent level set formulation for large-eddy simulation of premixed turbulent combustion. *Combust. Flame* (to appear).
- SIVASHINSKY, G. I. 1990 On the intrinsic dynamics of premixed flames. *Philos. Trans. R. Soc. London A* **332**, 135-148.